Paul Arellano, Kevin Tansey, Heiko Balzter and Doreen S. Boyd (accepted) Detecting the effects of hydrocarbon pollution in the Amazon forest using hyperspectral satellite images. *Environmental Pollution*.

This is the final accepted version of the above article and has been deposited according to guidelines: http://www.sherpa.ac.uk/romeo/issn/0269-7491/. The final published version (Arellano, P., Tansey, K., Balzter, H. and Boyd, D.S. (2015) Detecting the effects of hydrocarbon pollution in the Amazon forest using hyperspectral satellite images. *Environmental Pollution*, 205, 225-239) can be found at doi:10.1016/j.envpol.2015.05.041.

Detecting the effects of hydrocarbon pollution in the Amazon forest using hyperspectral satellite images

Paul Arellano[a,b,1], Kevin Tansey[a], Heiko Balzter[a,c] and Doreen S. Boyd[d]

[a] University of Leicester, Department of Geography, Centre of Landscape and Climate Research, University Road, Leicester, LE1 7RH, UK

[b] YachayTech University, School of Geological Sciences & Engineering, Urcuqui, Ecuador

[c] National Centre for Earth Observation, University of Leicester, University Road, Leicester, LE1 7RH, UK

[c] University of Nottingham, School of Geography, Nottingham, UK

Corresponding author: Paul Arellano, University Road, Bennett Building, LE1 7RH, Leicester, UK, (pa134@le.ac.uk or parellano@yachaytech.edu.ec)

Keywords: Petroleum pollution, hyperspectral remote sensing, Amazon forest, vegetation indices, Yasuni National Park

ABSTRACT

The global demand for fossil energy is triggering oil exploration and production projects in remote areas of the world. During the last few decades, hydrocarbon production has caused pollution in the Amazon forest inflicting considerable environmental impact. Until now it is not clear how hydrocarbon pollution affects the health of the tropical forest flora. During a field campaign in polluted and pristine forest, more than 1100 leaf samples were collected and analysed for biophysical and biochemical parameters. The results revealed that tropical forests exposed to hydrocarbon pollution show reduced levels of chlorophyll content, higher levels of foliar water content and leaf structural changes. In order to map this impact over wider geographical areas, vegetation indices were applied to hyperspectral Hyperion satellite imagery. Three vegetation indices (SR, NDVI and $NDVI_{705}$) were found to be the most appropriate indices to detect the effects of petroleum pollution in the Amazon forest.

---

[1] Present addess: YachayTech University, San Miguel de Urcuqui, Ibarra, Ecuador, Tlf: 593-983-033-541, pa134@le.ac.uk, parellano@yachaytech.edu.ec

Capsule:

Biophysical and biochemical alterations of vegetation of the Amazon forest caused by petroleum pollution can be detected from space using hyperspectral remote sensing.

1. Introduction

Global demand for energy is trigging oil and gas exploration and production across the Amazon basin, with even very remote areas leased out or under negotiation for access (Finer et al. 2008). In western Amazonia, there has been an unprecedented rise in this activity, causing environmental pollution in vast regions of forest via oil spills from pipelines networks and leakages from unlined open pits (Hurtig&San-Sebastián 2005, Bernal 2011). In some cases this has led to legal actions by local residents against international oil companies (Bernal 2011, Rochlin 2011). Currently in Ecuador the petroleum industry and its environmental/social interactions are at the centre of controversy since very sensitive regions and protected areas of this Amazon forest are under exploration and production (Marx 2010, Martin 2011, Vallejo et al. 2015).

Despite high international public interest in protecting Amazon rainforests, little scientific attention has focussed on the effects of oil pollution on the forest; much focus is on threats from deforestation, selective logging, hunting, fire and global and regional climate variations (Malhi et al. 2008, Davidson et al. 2012, Asner et al. 2004). The high diversity and intrinsic complex biological interactions of tropical forests and their vast expanse challenge our understanding of the impact of oil on them. Data collected *in situ* in these forests are rare, most likely due to access issues. An alternative approach to measuring and monitoring oil contamination in tropical forests at suitable spatial and temporal scales is desirable. It is suggested here that satellite imaging spectrometry, which affords the collection of hyperspectral data of the environment, could be a way forward. In order to detect vegetated landscape contamination using imaging

spectrometry, environmental change as a result of contamination need to have a measurable impact upon the biochemical, and related biophysical properties (e.g., pigment concentration, leaf structural and leaf area), of the vegetation growing in that environment. Such properties measured using hyperspectral remotely sensed data may then be used as a proxy to contamination (Mutanga;Skidmore & Prins 2004).

Experimental data generated under controlled conditions have demonstrated that plants exposed to pollutants exhibit stress symptoms (Horvitz 1982, Smith;Colls & Steven 2005, Horvitz 1985) which manifest themselves primarily in lower levels of chlorophyll content. Stress levels do, however, depend on plant tolerance to both concentration and exposure period (Smith;Steven & Colls 2005, Noomen et al. 2006). There is now an increasing availability of hyperspectral remotely sensed data from space (Hyperion on board of Earth Observation EO-1; Compact High Resolution Imaging Spectrometer-CHRIS on board of PROBA-1) and more are imminent at the time of writing (e.g. Sentinel-2; Environmental Mapping and Analysis Program (EnMAP)). The development of techniques to utilise these data sets for the detection of specific pollutants in a tropical forest environment is necessary and forms the focus of this study. Approaches to using these data include the use of both broad- and narrow-band vegetation indices (e.g., (Blackburn 2007)) and red edge position location (e.g., (Dawson&Curran 1998)). Their success may vary between species and pollutant (Steven et al. 1990, Sims&Gamon 2002), however, previously these techniques have been used to detect vegetation contamination by heavy metals (Kooistra et al. 2003, Rosso et al. 2005), radioactive materials (Davids&Tyler 2003, Boyd et al. 2006), as well as hydrocarbons (Smith;Steven & Colls 2005, Jago;Cutler & Curran 1999, Noomen et al. 2008, Noomen&Skidmore 2009, Zhu et al. 2013) and herbicides (Dash&Curran 2006).

1.1 Vegetation stress caused by crude oil

Vegetation responds to stress conditions with long-term metabolic and morphological changes: these includ changes in the rate of photosynthesis, changes in the absolute and relative concentration of the photosynthetic pigment (chlorophyll a and b, carotenoids) and changes in leaf size, thickness and structure (Davids&Tyler 2003). Different plant species respond differently to a particular stressor. Furthermore, the nature, intensity and length to exposure are factors that define the stress level on the vegetation. Baker (1970) summarised several pieces of research related to the effects of crude-oil on plants and showed that the toxicity of petroleum oil depends on the concentration of unsaturated, aromatics and acids compounds: the higher their concentration, the more toxic the oil is for plants. Molecules of crude-oil can penetrate the plant through its leaf tissue, stomata, and roots. The rate of penetration depends on the oil type, the contact part (leaves, roots), time of exposure, thickness of the cuticle and the density of the stomata. After penetrating into the plant, the oil may travel into the intercellular space and possibly also into the vascular system. Cell membranes are damaged by the penetration of hydrocarbon molecules leading to the leakage of cell contents, and the possible entry of oil into the cells.

Plant transpiration, respiration and photosynthetic rates are affected by hydrocarbon pollution (Baker 1970). The effects of hydrocarbons in plants reduce plant transpiration rates. On the other hand, plant respiration may either decrease or increase depending on the plant species or the oil type. Hydrocarbons reduce the rate of photosynthesis, and the amount of reduction varies with the type and amount of oil and with the species of plant. Cell injury may be the principal cause of photosynthesis inhibition because hydrocarbons tend to accumulate in the chloroplasts, which explains the reduced levels of chlorophyll content in vegetation affected by hydrocarbons.

1.2 Vegetation stress and chlorophyll

The interaction between hydrocarbons and the soils reduces the amount of oxygen and increases the CO_2 concentration, soils turn acidic and minerals are mobilised. These changes affect the vegetation health (Noomen et al. 2006, Shumacher 1996, Yang 1999, van der Meer;Yang & Kroonenberg 2006). Controlled experiments in the laboratory, most of them being applied to crops, have demonstrated that plants exposed to hydrocarbons experience reduced levels of chlorophyll which is a key parameter to detect plant stress caused by hydrocarbons (Smith;Colls & Steven 2005, Smith;Steven & Colls 2005, Noomen&Skidmore 2009, Yang 1999, Smith;Steven & Colls 2004, Noomen 2007). It is not clear how hydrocarbons influence changes in biophysical and biochemical parameters of vegetation growing in natural environments. At present, there are no published studies that investigate the effects of hydrocarbons in vegetation of tropical forest in the Amazon region.

This paper demonstrates the suitability of satellite imaging spectrometry for the detection of contamination by oil of the forest in the Ecuadorian Amazon. EO-1 (Earth-Observation 1) Hyperion imagery is analysed with supporting field data on soils and foliar properties with an overriding objective of producing a map of the spatial pattern of forest contamination by oil.

2. Materials and methods

2.1. Study area and sites

Three study sites within Ecuadorian Amazon rainforest were investigated (Figure **1Error! Reference source not found.**). Two were located in the lowland evergreen secondary forest of Sucumbios province, in the Tarapoa region (0°11’ S, 76°20’ W). Due to their close proximity, both sites share soil types, weather and

anthropogenic influences. Site 1 (polluted) is located by an abandoned petroleum platform where open pits have been discharging crude oil to the environment, or leaching out as the pits degrade or overflow, for the past 15 years. Site 2 (non-polluted) is some distance from Site 1 and so not directly influenced by the oil pollution evident at Site 1. Site 3 (Pristine forest-Yasuni) is situated in the highly diverse lowland evergreen primary forest of the Orellana province, in the northern section of Ecuador's Yasuni National Park (0°41' S, 76°24' W). The forest has a species richness among the highest globally (Tedersoo et al. 2010) and are situated well away from any sources of crude oil (and other anthropogenic influences).

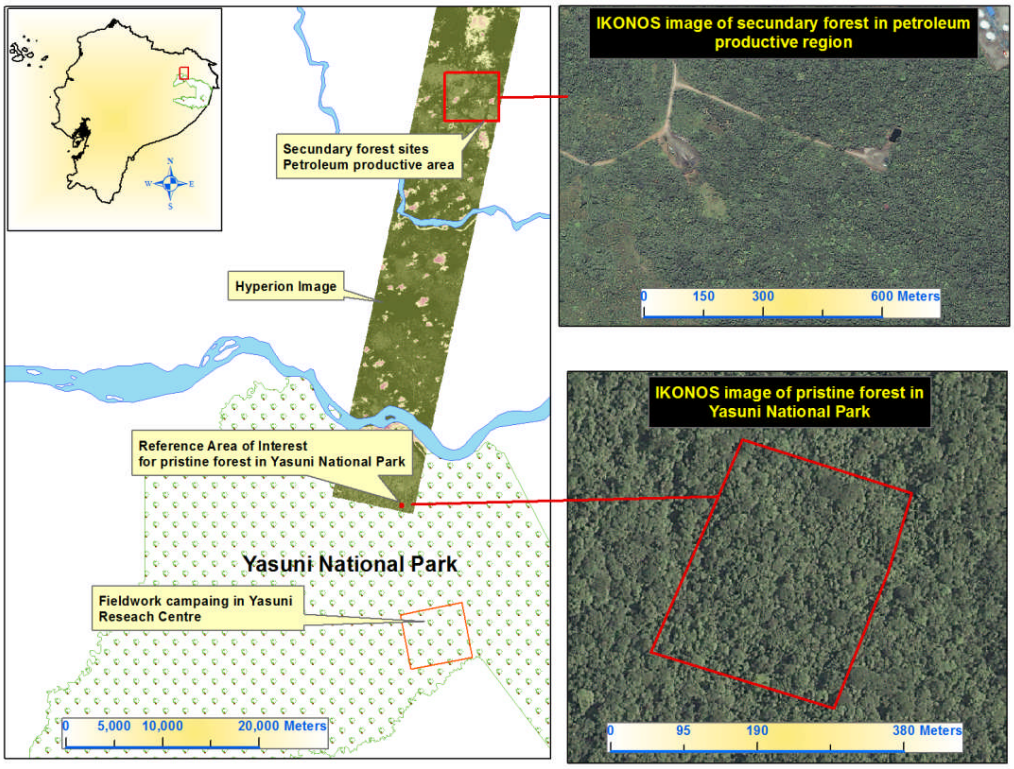

Figure 1. Location of the sampled sites in the Amazon region of Ecuador.

2.2. Site sampling and measurements

Fieldwork was undertaken from April to July 2012. From each of the three sites two sets of data were collected to measure any oil presence and potential contamination. One set focused on the measurement of levels of oil in the soil. Eight soil samples,

143 randomly situated, were collected at each of the three sites and several parameters
144 related to physical properties, nutrients, metals and hydrocarbons traces were analysed
145 in accredited laboratories following international standard methods (see Annex 1 for
146 details of soil sampling and results). The other set of data focused on measuring the
147 foliar biochemistry of leaves from the trees located at each site. At Site 1 all trees
148 located around the source of oil were sampled (388 samples); at Site 2 selectively
149 sampled areas located between 400 and 1250 meters from Site 1 were the focus of
150 measurement (124 samples); and in Site 3 accessible trees were sampled from 12
151 parcels of 20x20 m which covered an area of 4800 m^2 (545 samples). In total, therefore
152 1,057 trees were sampled (see Annex 2 and Annex 3 for a detailed description of the
153 plant family and specie sampled). From each tree well-developed branches, acquired
154 from different levels of the vertical forest profile using a telescopic pruner, tree-
155 climbing techniques and canopy towers, were sealed in large polyethylene bags and
156 stored in ice coolers.
157 Fully expanded mature leaves, with no herbivorous/pathogenic damage, were selected
158 from each of the collected branches and analysed. Each leaf was clipped at the midpoint
159 using cork borers to obtain a disk of known surface *(S)*; this is the optimal position from
160 which to take chlorophyll readings (Hoel 1998). Three SPAD-502 chlorophyll meter
161 readings were taken from each disk, at different positions, to compute a mean index
162 value. The fresh weight ***(Fw)*** and dry weight ***(Dw)*** of each leaf disk were then
163 calculated to measure (i) leaf water content (***Cw***) in g cm^{-2} = *(Fw-Dw)/S* (Gerber et al.
164 2011, Hunt Jr&Rock 1989, Datt 1999, Féret et al. 2011). Other leaf properties computed
165 were (ii) dry matter content (***Cm***) in g cm^{-2} = Dw/S (Gerber et al. 2011, Datt 1999, Féret
166 et al. 2011); (iii) Specific leaf area (***SLA***) in cm^2 g^{-1} = 1/Cm (Marenco;Antezana-Vera &
167 Nascimento 2009, White&Montes-R 2005, Vile et al. 2005, Sánchez-Azofeifa et al.

2009) ; (iv) Leaf water content (***LWC***) in % = (Fw-Dw)/Fw (Marenco;Antezana-Vera & Nascimento 2009); (v) Leaf dry matter content (***LDMC***) in % = Dw/Fw (Vile et al. 2005); and (vi) Leaf thickness or leaf succulence (***Lt***) in g cm^{-2} = 1/SLA*LDMC (Vile et al. 2005).

2.3. Hyperion image pre-processing

USGS EO-1 Hyperion image acquisition was requested for the time of the fieldwork campaign but cloudy conditions prevented new acquisitions, and therefore the only available Hyperion image was that acquired on 15th February 2005 and this was the focus of investigation. Hyperion data have a spatial resolution of $30m^2$ with each pixel covering the spectral range, 400-2500 nm. A single image is 7.65 km wide (cross-track) by 185 km long (along-track), and this meant that the single image available covered Sites 1 and 2 but not Site 3. Since Site 3 was located in a pristine, uncontaminated rainforest, a reference area of interest located 13km north from the sampled area was chosen inside the Yasuni National Park, with the assumption that the same forest conditions are present for comparative purposes (see Figure **1**). Since the Hyperion sensor operates from a satellite platform, pre-processing was undertaken to manage sensor and processing noise and retrieve reflectance for each waveband for use in subsequent analyses: pre-processing included waveband selection, atmospheric and smile effect corrections and noise reduction.

Wavelength selection: Hyperion data have 242 spectral bands; 51 bands are not radiometrically calibrated and consequently were not used (1 to 8 (visible); 58 to 78 (near infrared (NIR)) and 221-242 (shortwave infrared (SWIR)). Additionally, the 45 bands strongly affected by water absorption and noise were removed leaving a Hyperion data cube comprising 146 wavebands (Table 1).

Table 1. Selected usable bands of Hyperion image

Range (nm)	488-925	933	973-1114	1155-1336	1477-1790	1981-1991	2032-2355	**Total**
Bands	14-57	79	83-97	101-119	133-164	183-184	188-220	**146 usable bands**

The FLAASH atmospheric correction (ENVI 4.4) routine was applied to the data cube to remove the effects of the atmosphere and transform the raw radiance data ($Wm^{-2}\ sr^{-1}\mu m^{-1}$) to rescaled reflectance (%). Hyperion images provide effective measures of reflectance from the Earth surface if "smile effect" and random noise are managed. The "smile effect" refers to an across-track wavelength shift from the central wavelength, due to a change of dispersion angle with field position. In VNIR bands the shift range is between 2.6- to 3.5 nm, with the maximum shift occurring at column 256 in band 10. In SWIR bands, the spectral shift is less than 1 nm and is not significant for forest applications (Goodenough et al. 2003). The smile effect may affect Hyperion images in different degrees of the spectral range and may vary from scene to scene. Thus two methods developed by Dadon et al (2010) were employed to detect the smile effect in the Hyperion data cube. The first method uses the effects of the gas absorption features of O_2 around 760 nm (VNIR) and 2012 nm (SWIR) and the second method applies the Minimum Noise Fraction (MNF) transformation where the band MNF-1 showed a strong spatial gradient corresponding to the spectral smile. Subsequently, the "smile effect" was successfully removed by applying the approach developed by Datt et al (2003). This method relies in the significantly modified gain and offset values of columns affected by vertical stripes, therefore the statistical moments for each column are modified to match those for the whole image for each Hyperion band.

$$X'_{ijk} = \alpha_{ik}.X_{ijk} + \beta_{ik} \qquad (1.1)$$

Gains and offsets are computed by:

$$\alpha_{ik} = \frac{\overline{S}_{ik}}{S_{ik}} \quad (1.2)$$

$$\beta_{ik} = \overline{m}_{ik} - \alpha_{ik}.m_{ik} \quad (1.3)$$

Where:
m_{ik} = mean of the detector at *ith* column for band *k*.
$\overline{m}_{ik}$ = mean reference value.
S_{ik} = within column standard deviation.
$\overline{S}_{ik}$ = within column standard deviation reference value.

The method takes into account the reference mean to be the total image mean and the reference standard deviation to be the whole image within column standard deviation.

$$\overline{m}_{ik} = \overline{m}_{k} \quad (1.4)$$

$$\overline{S}_{ik} = \overline{S}_{k} \quad (1.5)$$

Noise reduction: Finally, the MNF (Minimum Noise Fraction) method was applied to reduce noise and data dimensionality. MNF is an algorithm used for ordering data cubes into components of image quality using a two-cascade-principal-components-transform which selects new components in order to decreasing signal to noise ratio (SNR) (Goodenough et al. 2011, Apan et al. 2004). In this study, forward MNF transformation was applied to the 146 usable bands of Hyperion cube and the result shown in Figure **2**a illustrates that most of the information (83%) is contained in the first 15 MNF bands represented by the higher eigenvalues. Figure **2**b shows the first MNF band which contains most of the information (43.6%) and Figure **2**c illustrates that MNF band 15 contains noise and little information. MNF bands between 16 and 146 basically contain noise (Datt et al. 2003). The next step was to apply the inverse MNF process to the 15 bands containing useful information in order to transform back to the 146 Hyperion spectral bands removing in this way the low SNR from the data.

Figure 3**Error! Reference source not found.** illustrates the Hyperion spectral signal after pre-processing steps.

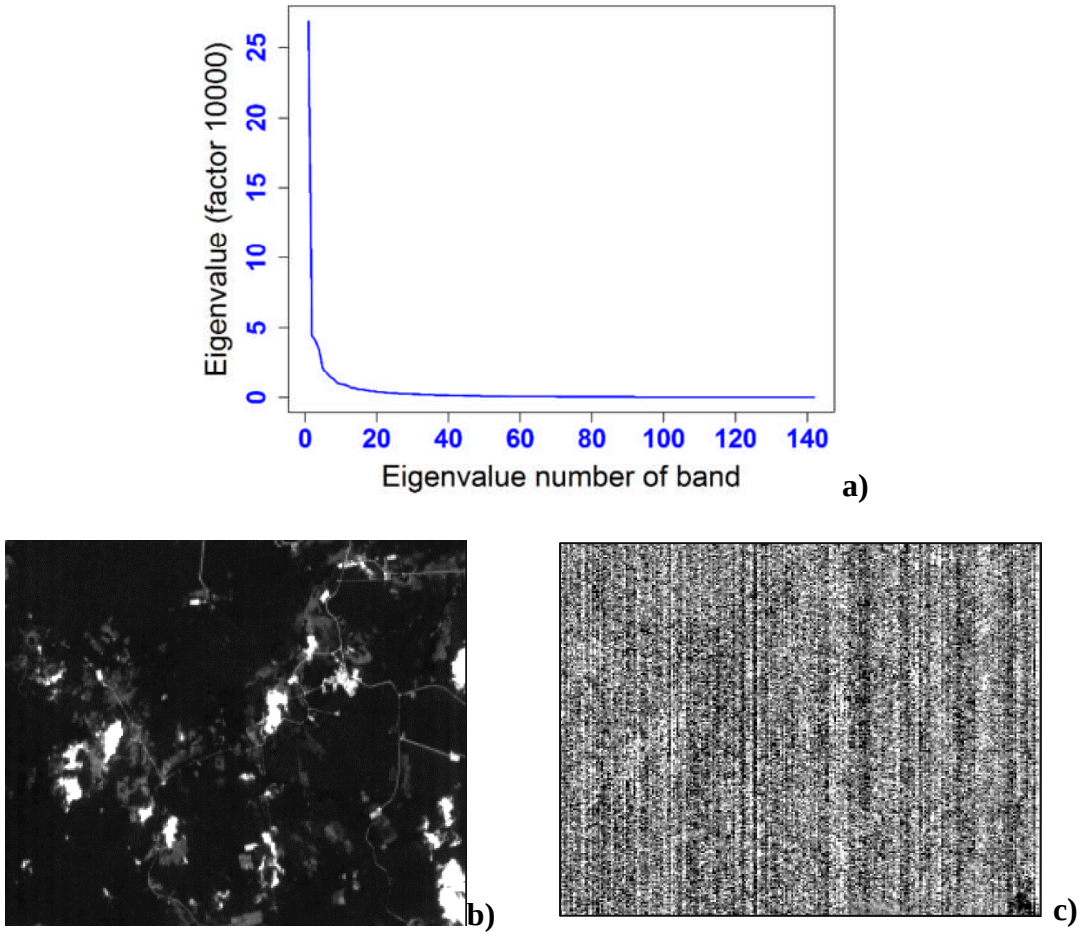

Figure 2. a) Eigenvalues for the 146 Hyperion spectral bands; b) MNF Band 1 containing most of the information (44%); c) MNF band 15 (0.9)

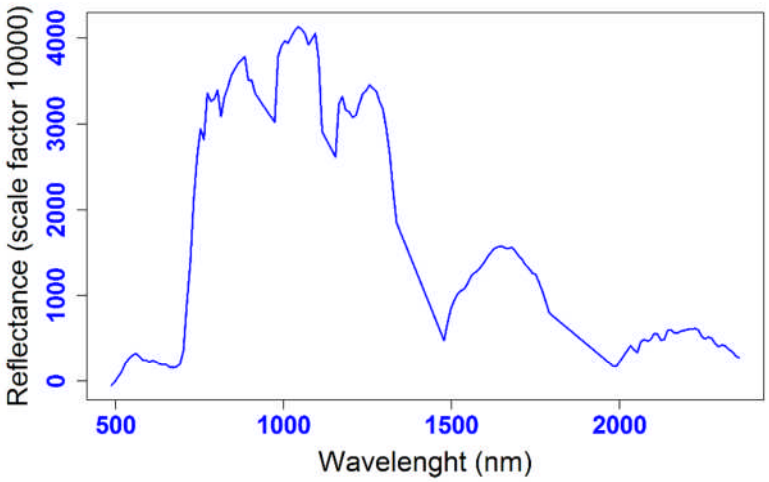

Figure 3. Resulting Hyperion spectral signal after pre-processing

2.4. Spectral vegetation indices (VI)

Several VI grouped in broad-band, narrow-band-greenness/chlorophyll, narrow-band-other pigments and narrow-band-water indices were computed (Table 2 and Annex 4 in Supplementary Materials) from the processed Hyperion data. From them, a total of 28 indices were selected. Some indices, like PRI (Photochemical Reflectance Index) (Gamon;Peñuelas & Field 1992) and CARTER 1 (Carter 1994) did not resolve appropriately when applied to our Hyperion data. Most of the non-applicable indices used reflectance values in the blue range of the spectrum where Hyperion data showed low SNR.

A value for every pixel covering each of the study sites was extracted for each vegetation index (in total Site 1 covers 18000 m^2 (20 pixels); Site 2 covers 14000 m^2 (16 pixels) and Site 3, 64800 m^2 (72 pixels)).

261 Table 2. Vegetation indices applied to Hyperion images in the study area

	INDEX	EQUATION	REFERENCES
BROAD-BAND INDICES			
1	Simple Ratio (SR)	$\frac{\rho_{NIR}}{\rho_{Red}}$	(Rouse;Haas & Schell 1974)
2	Normalised Difference Vegetation Index (NDVI)	$\frac{\rho_{NIR} - \rho_{Red}}{\rho_{NIR} + \rho_{Red}}$	(Rouse;Haas & Schell 1974)
3	Green Normalised Difference Vegetation Index (GNDVI)	$\frac{\rho_{NIR} - \rho_{Green}}{\rho_{NIR} + \rho_{Green}}$	(Gitelson;Kaufman & Merzlyak 1996)
4	Enhanced Vegetation Index (EVI)	$2.5\,\frac{\rho_{NIR} - \rho_{Red}}{\rho_{NIR} + 6\rho_{Red} - 7.5\rho_{Blue} + 1}$	(Huete et al. 1997)
5	Atmospherically Resistant Vegetation Index (ARVI)	$\frac{\rho_{NIR} - (2\rho_{Red} - \rho_{Blue})}{\rho_{NIR} + (2\rho_{Red} - \rho_{Blue})}$	(Kaufman&Tanre 1992)
NARROW-BAND INDICES: GREENES, CHLOROPHYLL, REP			
6	Sum Green (SG)	$\sum_{600nm}^{500nm} \rho_{Green}$	(Gamon&Surfus 1999)
7	Pigment Specific Simple Ratio-Chl (PSSRa)	$\frac{\rho_{800}}{\rho_{680}}$	(Blackburn 1998)()
8	Red-Edge Normalised Difference Index ($NDVI_{705}$)	$\frac{\rho_{750} - \rho_{705}}{\rho_{750} + \rho_{705}}$	(Sims&Gamon 2002)
9	Modified Red-Edge Simple Ratio (mSR_{705})	$\frac{\rho_{750} - \rho_{445}}{\rho_{705} + \rho_{445}}$	(Sims&Gamon 2002)
10	Modified Red-Edge Normalised Difference Index ($mNDVI_{705}$)	$\frac{\rho_{750} - \rho_{705}}{\rho_{750} + \rho_{705} + 2\rho_{445}}$	(Sims&Gamon 2002)
11	Carter Index 2 (CTR2)	$\frac{\rho_{695}}{\rho_{760}}$	(Carter;Cibula & Miller 1996)
12	Lichtenthaler Index 1(LIC1) or Pigment Specific Normalised Difference – Chla (PSNDa)	$\frac{\rho_{800} - \rho_{680}}{\rho_{800} + \rho_{680}}$	(Blackburn 1998, Lichtenthaler et al. 1996)
13	Optimised Soil-Adjusted Vegetation Index (OSAVI)	$1 + 0.16\frac{\rho_{800} - \rho_{670}}{\rho_{800} - \rho_{670} + 0.16}$	(Rondeaux;Steven & Baret 1996)
14	Modified Chlorophyll Absorption Ratio Index (MCARI)	$\frac{\rho_{700}}{\rho_{670}}[(\rho_{700} - \rho_{670}) - 0.2\,(\rho_{700} - \rho_{550})]$	(Daughtry et al. 2000)
15	Ratio of derivatives at 725 and 702 nm ($Der_{725\text{-}702}$)	$\frac{d\rho/d\lambda_{725}}{d\rho/d\lambda_{702}}$	(Smith;Steven & Colls 2004)
16	Red-Edge Position (REP)	$\rho_{re} = \frac{\rho_{670} + \rho_{780}}{2}$ $700 + 40\frac{\rho_{re} - \rho_{700}}{\rho_{740} - \rho_{700}}$	(Guyot;Baret & Major 1988)
17	Vogelmann Red-Edge Index (VOG1)	$\frac{\rho_{740}}{\rho_{720}}$	(Vogelmann;Rock & Moss 1993)
18	Chlorophyll Index (CI_{590})	$\frac{\rho_{880}}{\rho_{590}} - 1$	(Gitelson&Merzlyak 1997)
19	MERIS Terrestrial Chlorophyll Index (MTCI)	$\frac{\rho_{753.75} - \rho_{708.75}}{\rho_{708.75} - \rho_{681.25}}$	(Curran&Dash 2005)

NARROW-BAND INDICES: OTHER PIGMENTS			
20	Structure Insensitive Pigment Index (SIPI)	$\frac{\rho_{800}-\rho_{445}}{\rho_{800}-\rho_{680}}$	(Penuelas et al. 1995)
21	Red Green Ratio (RG)	$\frac{\sum \rho_{Red}}{\sum \rho_{Green}}$	(Gamon&Surfus 1999)
22	Anthocyanin Reflectance Index 1 (ARI1)	$\frac{1}{\rho_{550}}-\frac{1}{\rho_{700}}$	(Gitelson;Merzlyak & Chivkunova 2001)()
23	Anthocyanin Reflectance Index 2 (ARI2)	$\rho_{800}\left[\frac{1}{\rho_{550}}-\frac{1}{\rho_{700}}\right]$	(Gitelson;Merzlyak & Chivkunova 2001)
NARROW BAND INDICES: WATER			
24	Water Band Index (WBI)	$\frac{\rho_{900}}{\rho_{970}}$	(Peñuelas et al. 1997)
25	Normalised Difference Water Index (NDWI)	$\frac{\rho_{857}-\rho_{1241}}{\rho_{857}+\rho_{1241}}$	(Gao 1996)
26	Moisture Stress Index (MSI)	$\frac{\rho_{1599}}{\rho_{819}}$	(Hunt Jr&Rock 1989)
27	Normalised Difference Infrared Index (NDII)	$\frac{\rho_{819}-\rho_{1649}}{\rho_{819}+\rho_{1649}}$	(Hardisky;Klemas & Smart 1983)
28	Normalised Heading Index (NHI)	$\frac{\rho_{1100}-\rho_{1200}}{\rho_{1100}+\rho_{1200}}$	(Pimstein et al. 2009)

2.5. Data analysis

The mean and standard deviation was calculated for all data generated for each site (both field- and imagery-based). To assess whether there has been any oil pollution on the forest it is expected that there will be a statistically significant difference in the levels of contaminant in the soil between the sites and that being so, any corresponding statistical difference present in the vegetation indices could ultimately be used to determine pollution from space and presented as a map of contamination. This difference was determined using an ANOVA. Those vegetation indices exhibiting a significant difference in the ANOVA at 99.9% confidence level ($p<0.001$) were then used in a post-hoc pairwise comparison using the adjustment method of Holm (see Table **4**) to determine the pairwise significant differences between sites. Those indices exhibiting strongly significant differences between sites were used to map an area of 52 km^2 which covered a petroleum production region. A threshold was determined for each

of the selected vegetation indices based on the median and the min/max value which better characterises the area affected by oil pollution. Based on the threshold values, a mask was created for each vegetation index. An image of vegetation contamination was computed by summing the masks such that a pixel value having the value that equalled the sum of the number of vegetation indices used is one containing contaminated forest.

3. Results

3.1. Analysis of field-derived data

The results of the soil analysis (presented in Annex 1-Supplementary Materials) showed that Site 1 (polluted) had high levels of Total Petroleum Hydrocarbon (TPHs), near 9000 mg/kg. All the soils sampled at Sites 2 (non-polluted) and Site 3 (Pristine forest-Yasuni) reported values lower than 200 mg/kg which confirms that these two sites were not affected by hydrocarbons pollution (Figure **4**).

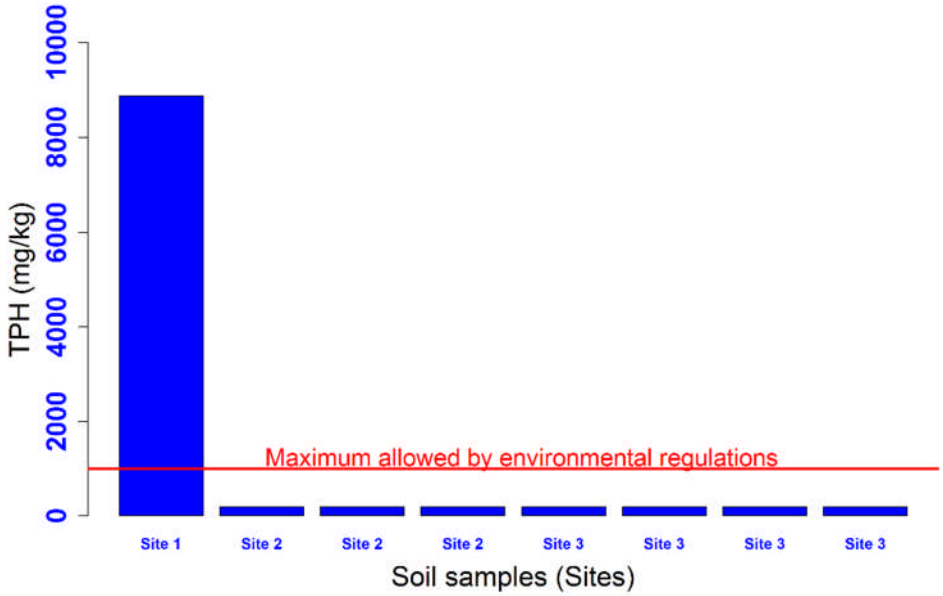

Figure 4. Results of TPHs (Total Petroleum Hydrocarbons) for the study sites compared with the environmental regulation threshold established by the Environmental Ministry of Ecuador.

3.2. Analysis of foliar biophysical and biochemical parameters

Initial focus on the plotted means and ±95% confidence intervals for each foliar biochemical/biophysical variable (Figure 5. Mean and ±95% confidence interval for the foliar biophysical and biochemical parameters

; descriptive statistics presented in Annex 5 of Supplementary Materials), and the ANOVA and associated pairwise comparisons via the Holm method (Table 3), was on how different site 1 (polluted) was from sites 2 and 3. The chlorophyll content (C_{ab}) was significantly lower at site 1 with values strongly different (99.9%) to those for the two non-polluted sites (2 and 3). No significant difference in chlorophyll content was evident between the two unpolluted sites. Leaf water content (*LWC*) and Leaf dry matter content (*LDMC*) also exhibited strongly significant differences (99.9%) between the unpolluted site 1 and sites 2 (strongly significant at 99.9%) and 3 (highly significant at 99%). Total water content (*Cw*) difference however had a slightly different pattern with differences observed between site 1 and 2 only significant at 95% level but highly significant (at 99.9%) between site 1 and site 3.

Organic matter content (*Cm*) was significantly different (95%) between Site 1 and 2 but insignificant in difference between Site 1 and 3, with a high (99%) level of significance difference being shown between the two unpolluted sites. Leaf thickness (*Lt*) was strongly significantly different (99.9%) between Site 1 and 3 but no difference was observed between Sites 1 and 2 for this foliar property. No differences in SLA were observed between any of the sites.

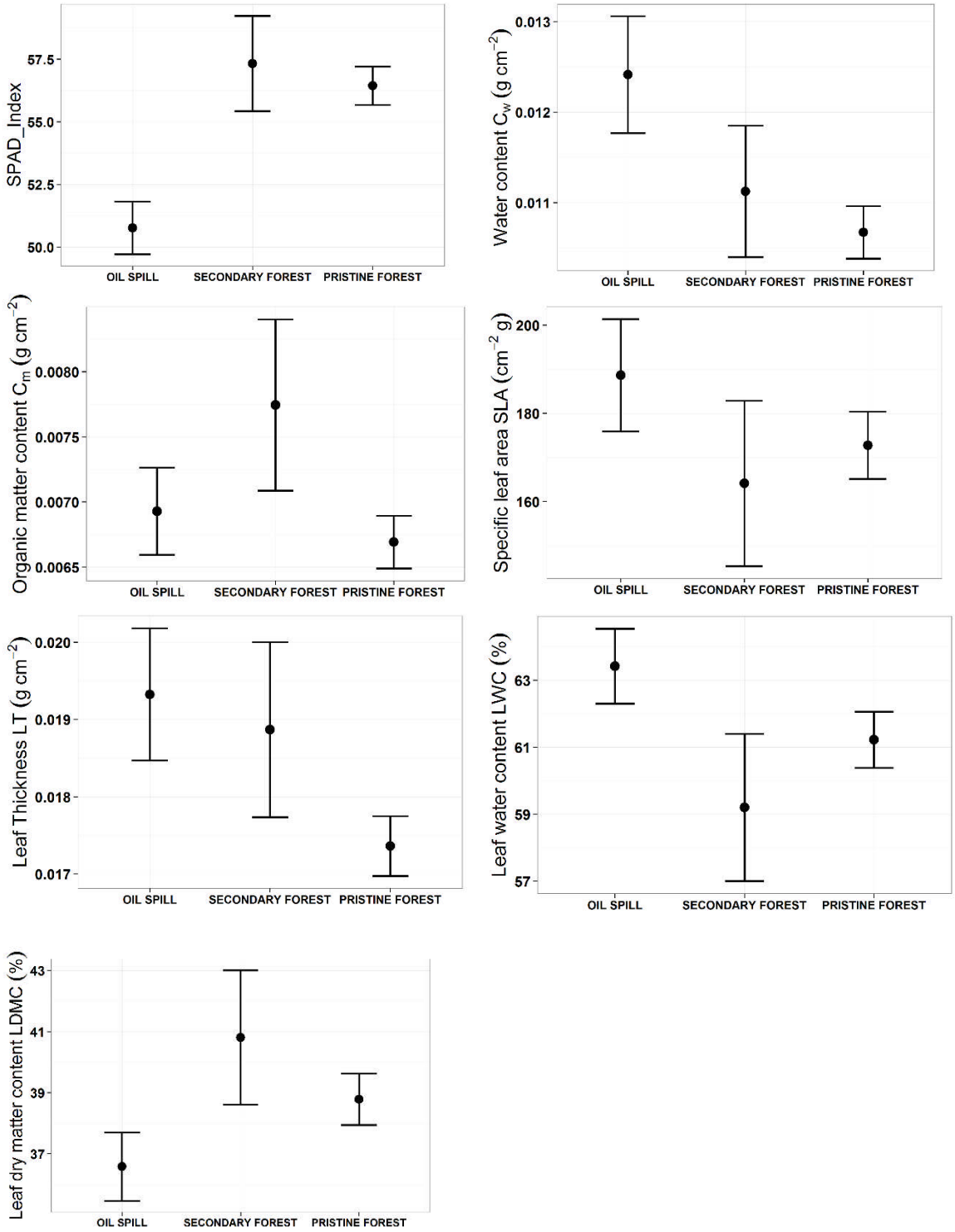

313 Figure 5. Mean and ±95% confidence interval for the foliar biophysical and biochemical
314 parameters
315

316 Table 3. Pairwise comparison of p-values with holm adjustment method

	C_{ab}	Cw	Cm	SLA	Lt	LWC	LDMC
ANOVA test	2.0E-16	4.2E-07	1.7E-03	2.8E-02	2.2E-05	1.5E-05	1.5E-04
	***	***	**	*	***	***	***

Pairwise comparison – Holm adjustment method							
Oil spill (Site 1)- No Polluted (Site 2)	6.2E-10 ***	2.1E-02 *	1.5E-02 *	7.8E-02	5.0E-01	4.4E-04 ***	4.4E-04 ***
Oil spill (Site 1)- Pristine forest (Site 3)	1.2E-14 ***	2.2E-07 ***	2.3E-01	7.8E-02	2.0E-05 ***	4.2E-03 **	4.2E-03 **
No polluted (Site 2)- Pristine forest (Site 3)	2.1E-01	3.5E-01	1.1E-03 **	4.2E-01	4.3E-02 *	5.8E-02	5.8E-02
*** Strongly significant (99.9%) ** Highly significant (99%) * Significant (95%) No significant difference							

3.3. Analysis of vegetation indices from Hyperion images

Means and standard deviations obtained for each set of vegetation indices are shown in Figure 6 (broadband), Figure 7 (greenness, chlorophyll, REP), Figure 8 (other pigments) and Figure 9 (water indices). The corresponding pairwise comparisons via the Holm method are presented in Table 4.

Most vegetation indices (23 of the 28) illustrated 99.9% significance difference between Site 1 (polluted) and Site 3 (pristine forest) which are the most dissimilar sites in terms of forest structure, plant species and conservation. 16 of 28 indices showed 99.9% significance differences between Site 2 (secondary non-polluted forest) and Site 3 (pristine forest) and just 11 vegetation indices registered 99.9% significance between Site 1 (polluted) and Site 2 (non-polluted forest). Of those 11 vegetation indices which were able to discriminate as strongly significant (99.9%) the difference between the two sampled secondary forests (Site 1 and Site 2), all of them corresponding to broad-band indices and narrow-band-greenness-chlorophyll-red-edge index groups. Lower and no-significance were found in indices grouped under other pigments and water indices. Annex 6, Annex 7 and Annex 8 in the Supplementary Material section present the descriptive statistics for each vegetation index applied and for each study site.

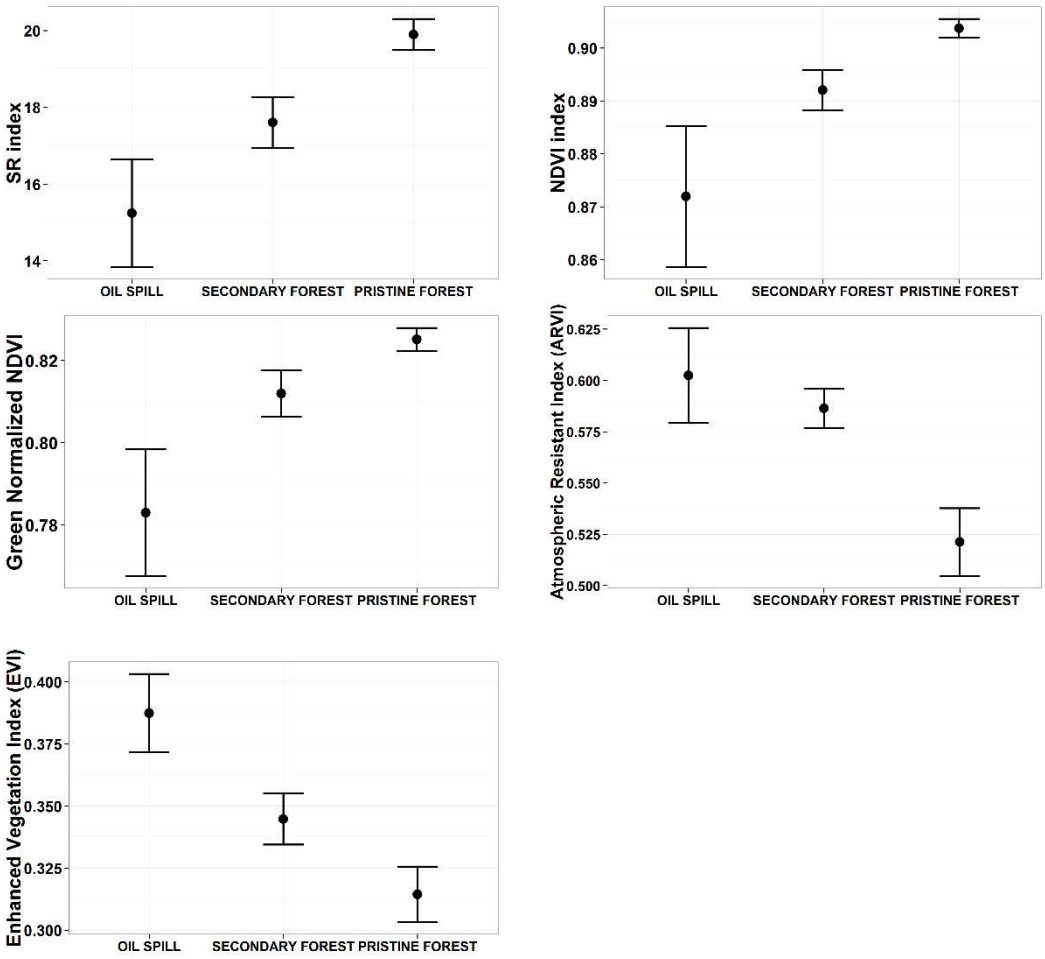

334 Figure 6. Mean and ±95% confidence interval of the calculated Broad-band vegetation
335 indices

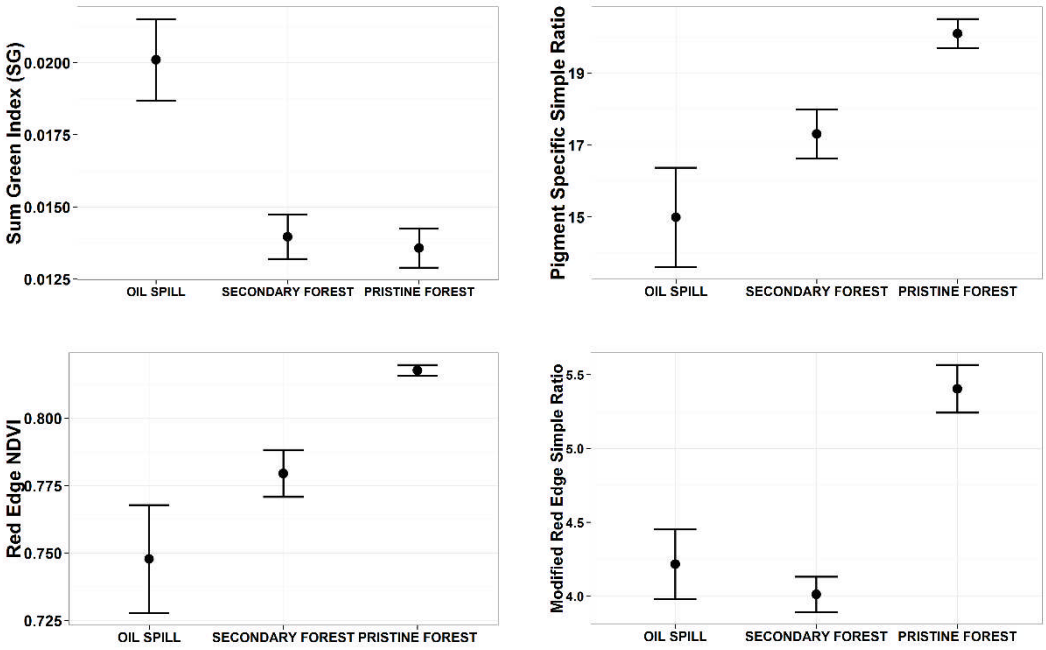

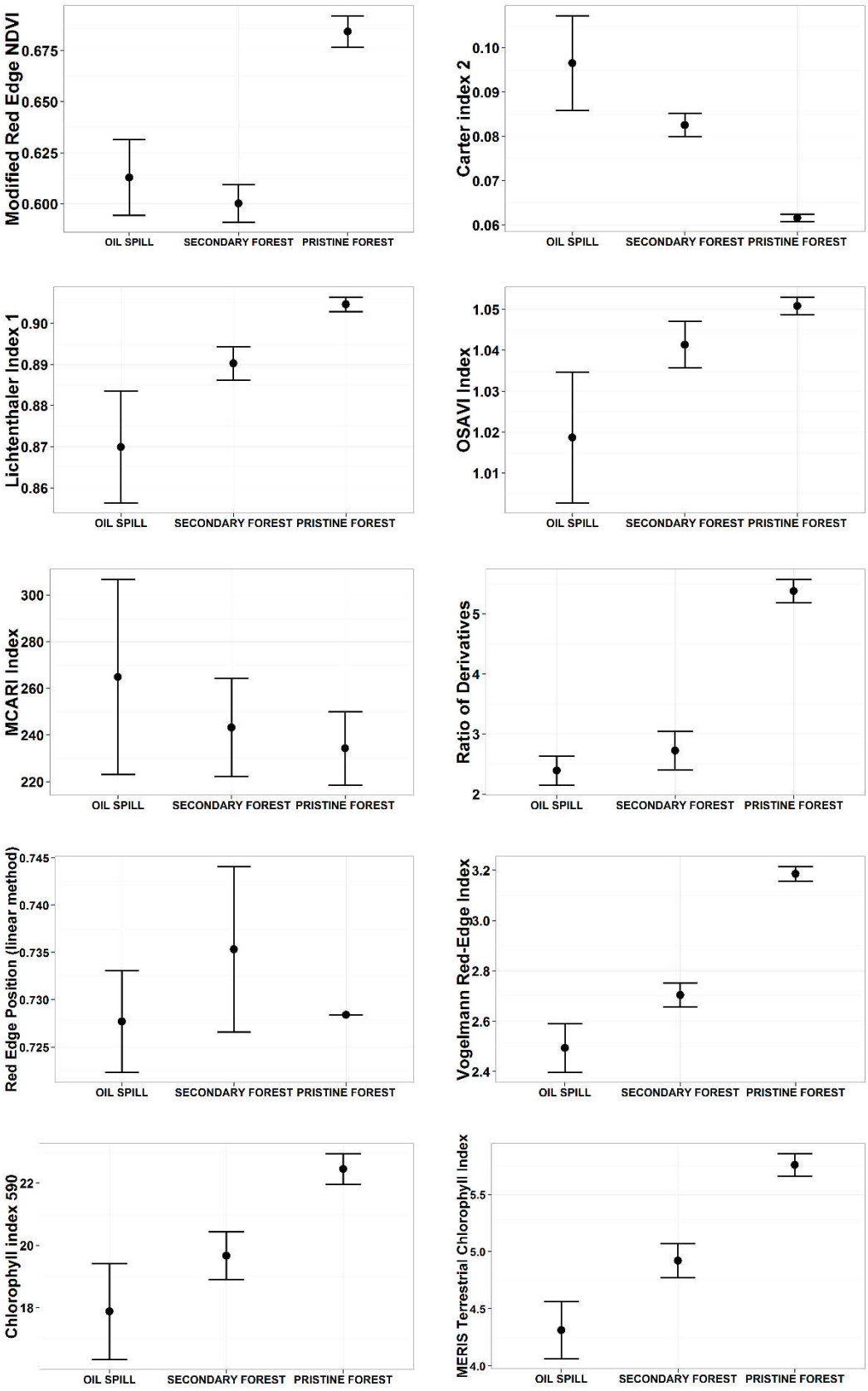

336 Figure 7. Mean and ±95% confidence interval of the calculated Narrow-Band
337 Vegetation Indices: Greenness / Chlorophyll indices
338

339

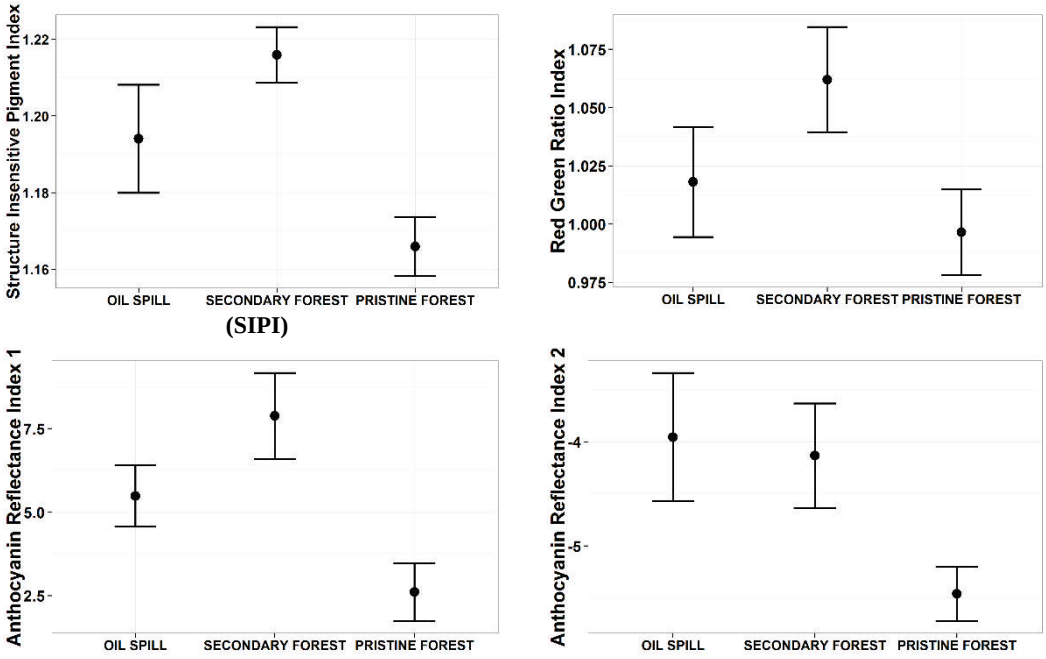

340 Figure 8. Mean and ±95% confidence interval of the calculated Narrow-Band
341 Vegetation Indices: Other pigments
342

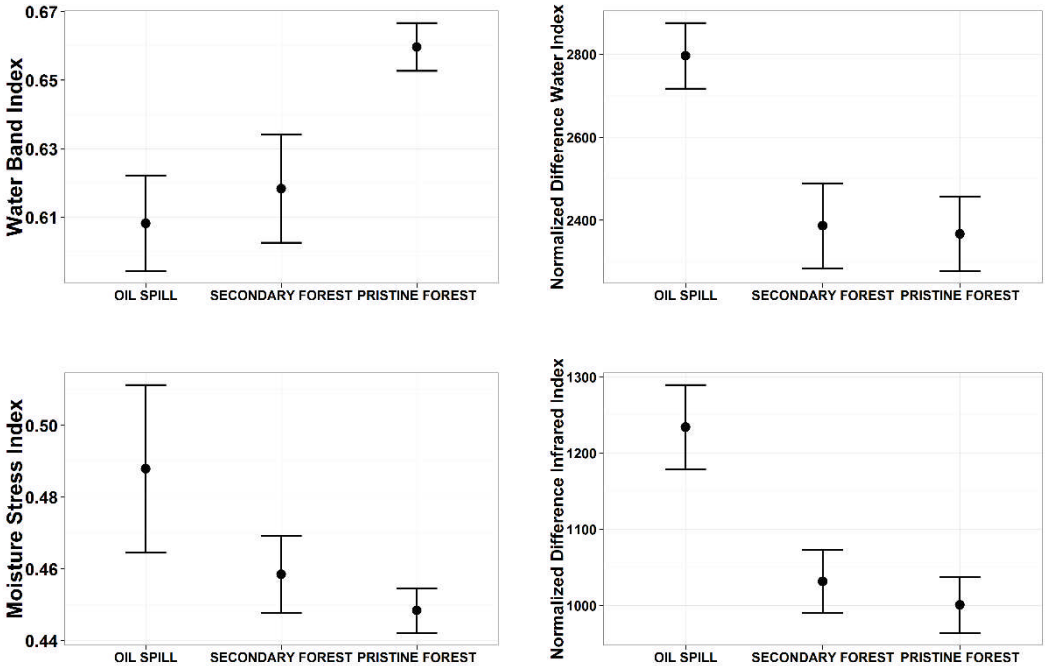

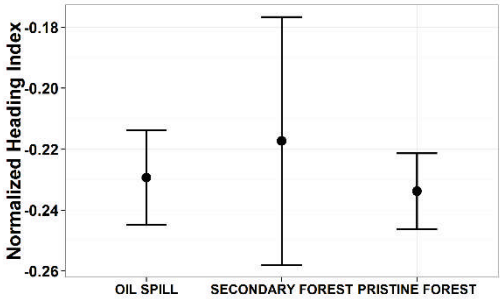

343 Figure 9. Mean and ±95% confidence interval of the calculated Narrow-Band
344 Vegetation Indices: Water Indices
345

346 Table 4. Analysis of variance and pairwise comparison of means using Holm
347 adjustment method for the study sites (oil pollution, secondary forest and pristine forest)

	INDEX	Site 1 (polluted) vs. Site 2 (non-polluted)	Site 1 (polluted) vs. Site 3 (pristine forest)	Site 2 (non-polluted) vs. Site 3 (pristine forest)
BROAD-BAND VEGETATION INDICES				
1	SR	***	***	***
2	NDVI	***	***	**
3	GNDVI	***	***	**
4	ARVI	ns	***	***
5	EVI	**	***	*
NARROW-BAND VEGETATION INDICES				
GREENNESS / CHLOROPHYLL				
6	SG	***	***	ns
7	PSSRa	***	***	***
8	$NDVI_{705}$	***	***	***
9	mSR_{705}	ns	***	***
10	$mNDVI_{705}$	ns	***	***
11	CRT2	***	***	***
12	LIC1 or PSNDa	***	***	**
13	OSAVI	***	***	*
14	MCARI	ns	ns	ns
15	$Der_{725-702}$	ns	***	***
16	REP	**	ns	**
17	VOG1	***	***	***
18	CI_{590}	*	***	***
19	MTCI	***	***	***
OTHER PIGMENTS				
20	SIPI	*	***	***
21	RG	ns	ns	**
22	ARI1	*	**	***
23	ARI2	ns	***	***
WATER INDICES				
24	WBI	ns	***	***
25	NDWI	.	***	*
26	MSI	*	***	ns

27	NDII	ns	***	***
28	NHI	ns	ns	ns
******* Strongly significant (0.1%) ****** Highly significant (1%) ***** Significant (5%) **.** Lowest significant (10%) ns No significant				

348

349 ***3.4. Mapping vegetation stress***

350 The eleven vegetation indices that strongly discriminated polluted and non-
351 polluted secondary forests (strongly significant at 0.1% level of confidence - see Table
352 **4**) were selected as the more sensitive indices to detect the effects of petroleum
353 pollution. Thresholds were defined based on the median and the min/max values of the
354 oil spill site (see Table 5 and Supplementary Materials, Annex 9). Based on those
355 thresholds, a map (Figure 10) illustrate the locations of contaminated forest was
356 produced (effect). Also mapped is the infrastructure for petroleum extraction: platforms,
357 stations, oil pipelines and roads (cause). In the majority of cases the cause and effect are
358 spatially coincident.

359

360 Table 5. Threshold values defined for selected vegetation indices in the site affected by
361 hydrocarbon pollution

Index	**Median**	**Min/Max value**
SR	16.3065	8.5502 (min.)
NDVI	0.8844	0.7906 (min.)
GNDVI	0.7987	0.7096 (min.)
SG	0.0193	0.0278 (max.)
PSSRa	16.0014	8.3391 (min.)
$NDVI_{705}$	0.7620	0.6351 (min.)
CTR2	0.08669	0.1603 (max.)
LIC1	0.8844	0.7906 (min.)
OSAVI	1.0290	0.9284 (min.)
VOG1	2.5724	2.0433 (min.)
MTCI	4.4889	3.0824 (min.)

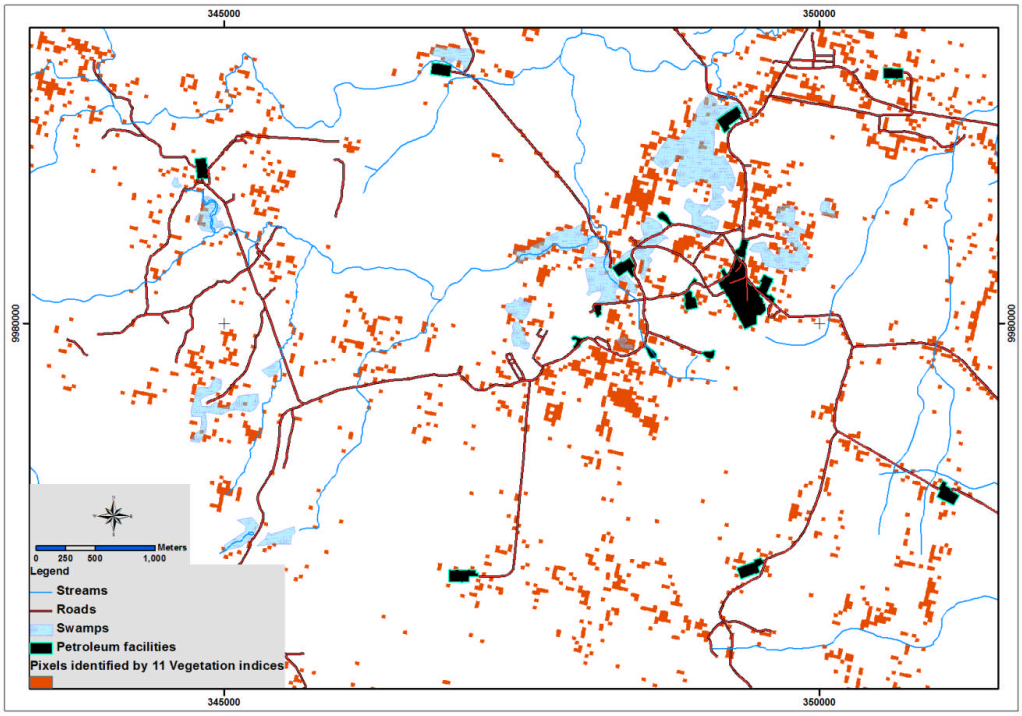

Figure 10. Areas identified as vegetation stress based on the eleven vegetation indices.

To ascertain the importance of each the 11 VI in the mapping of contamination a discriminant function analysis was undertaken which illustrates that three VI (the SG, NDVI and $NDVI_{705}$) explain 83% of the ability to separate between the 3 sites (Table 6). Figure 11 remaps contamination based on these 3 VI only showing a close agreement with Figure 10. By way of validation Figure 12 depicts those sites sampled in the field that have been correctly allocated as either contaminated or uncontaminated. This Figure also affords closer examination of the cause and effect of the hydrocarbon contamination in these forests.

Table 6. Results of discrimination function analysis

Vegetation indices	LD1	LD2	Relative weight (LD1)
SG	592.0	-735.9	53.0%
NDVI	-241.2	115.5	21.6%
$NDVI_{705}$	94.1	18.7	8.4%
CTR2	51.7	-23.7	4.6%
GNDVI	-51.1	-146.7	4.6%
LIC1	39.3	5.9	3.5%
VOG1	27.4	24.5	2.4%

OSAVI	-9.8	-22.6	0.9%
MTCI	-3.7	-4.8	0.3%
PSSRa	3.5	1.9	0.3%
SR	-2.6	-3.2	0.2%
Trace proportion (variance)	95.0% between	5.0% within sites	
Eigenvalues	69.3	16.0	

374

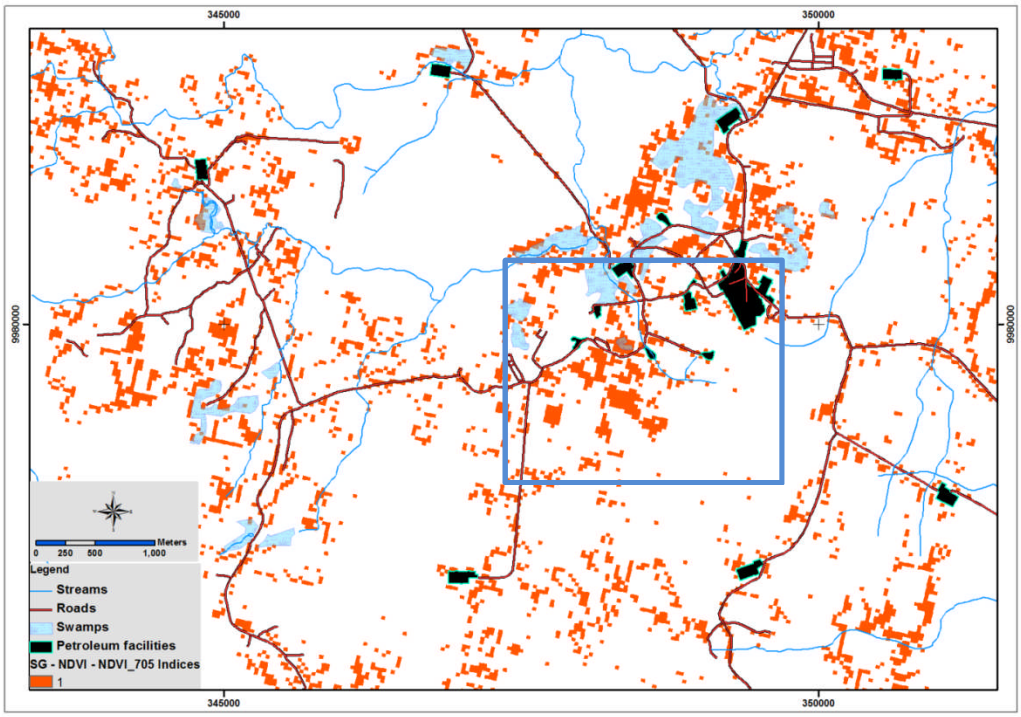

375

376 Figure 11. Areas identified as vegetation stress based on the SG, NDVI and NDVI_705
377 indices which together contribute to 83% of the site separability. The blue square is that
378 highlighted in Figure 10.

379

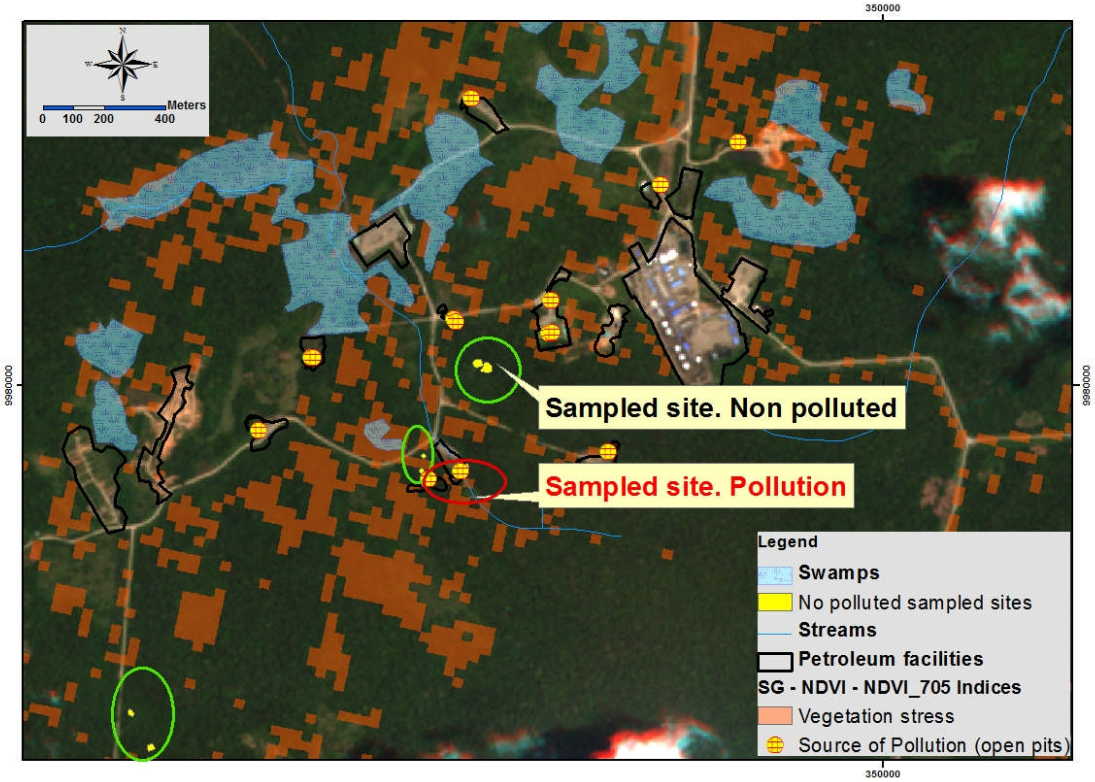

Figure 12. Areas detected as vegetation stress in petroleum productive area. Open pits identified as source of pollution and RAPIDEYE images (background) have been provided by the Environmental Ministry of Ecuador (PRAS-program)

4. Discussion

4.1. Petroleum contamination in soil

The soil analyses of this study revealed a latent effect of the formerly disposed hydrocarbons at Site 1. Since the environmental regulations in Ecuador state the maximum level of TPHs for sensible ecosystems to be 1000 mg/kg (Ministerio de Energia y Minas 2001) it is clear that this site is affected by petroleum pollution. Other sources of pollution identified as open pits and facilities where polluted soils have been stocked for remediation have been identified by environment audits and studies carried out by the Environmental Ministry of Ecuador (Environmental Ministry of Ecuador 2014). At those sites crude oil has been exposed to the environment and although lighter hydrocarbons (gaseous) have evaporated and biodegraded, liquid hydrocarbons have migrated from the open pits by infiltration into the soil and dissolution in water

(Environmental Ministry of Ecuador 2005, Environmental Ministry of Ecuador 2009). Any vegetation in close proximity has thus potential to be impacted. Water transports pollutants away from its source, which are subsequently deposited in the nearby swamps to accumulate. This also impacts on the vegetation. This was particularly evident in Figure 10 and Figure 12 where a cluster of pixels identified as stressed vegetation is located around swamps. As expected, sites 2 and 3 had no soil contamination, being located away from sources of petroleum production.

4.2. Impact of petroleum contamination on leaf properties

Of the leaf biochemical and biophysical properties measured it was chlorophyll content and those associated with water content that exhibited significant differences between the polluted site and non-polluted sites. The low levels of chlorophyll content seen at site 1 indicate vegetation stress caused by a reduction of photosynthetic activity in vegetation exposed to petroleum contaminant. The C_{ab} content is responsive to a range of stresses on vegetation because of its direct role in the photosynthetic processes of light harvesting and initiation of electron transport (Zarco-Tejada et al. 2000). The higher values of water content (*Cw*) observed at the polluted site may be linked to the adaptation process of plants to close the stomata under stress conditions as strategy to reduce transpiration, which in turns reduce photosynthetic rate linked to the lower chlorophyll and thus total tree metabolism (Larcher 2003, Zweifel;Rigling & Dobbertin 2009). Other foliar properties related to water, those expressed on mass basis (% LWC and % LDMC) also differed and is due to the fact that as these parameters are not normalised by the leaf area, these differences can be explained by the high species diversity of the sample sites where leaves vary greatly in morphology, anatomy and physiology in response to their growing conditions (Tedersoo et al. 2010). Of these leaf variables, it is chlorophyll content that lends itself to be measured from space using a

hyperspectral sensor, and since it is this that showed differences between the polluted and unpolluted sites, this suggests that by measuring this biochemical in vegetation compartments, detection of petroleum contamination across vast expanse of tropical forests is indeed possible.

Other studies have suggested leaf thickness to be a useful indicator of vegetation stress. Either as a result of increased levels of foliar water content per unit area and/or a shift of species composition. Indeed, some species may be replaced by invasive species which are more resistant to the petroleum influence (Noomen;van der Werff & van der Meer 2012). However, here leaf thickness showed no significant difference between the oil spill secondary and non-oil spill secondary so this is inconclusive and not a clear variable to measure from space.

4.3. Vegetation indices to detect the occurrence of petroleum pollution

As suggested by the field data it was those vegetation indices with sensitivity to photosynthetic pigments that were most useful in discriminating between the contaminated and non-contaminated sites. The Sum Green vegetation index (SG) clearly identified an increased reflectance signal in the visible spectral region of the area affected by petroleum pollution which confirms the sensitivity of Hyperion image to register reduced chlorophyll content levels in the polluted site. Also of use are the broad-band and narrow-band vegetation indices related to the traditional NDVI (SR, GNDVI, NDVI705), endorsing the conclusions of (Zhu et al. 2013).

Two narrow-band indices developed to estimate chlorophyll content across species (PSSRa and $NDVI_{705}$) clearly exhibited lower chlorophyll content for the tropical forest affected by petroleum. However, this contradicts Sims and Gamon's (2002) conclusions which suggested that PSSRa was largely insensitive to variations in chlorophyll content in a multispecies forest. Conversely, this study agrees with their

findings related to the sensitive of $NDVI_{705}$ to variations of chlorophyll content across several species. The narrow-band indices $NDVI_{705}$, CTR2, LIC1 and OSAVI also showed strong significant differences between sites, concurring with those who used these indices for detecting vegetation impacted by natural hydrocarbon gases leakage (Noomen&Skidmore 2009). VOG1 and MTCI indices explore the relationship between REP and foliar chlorophyll content also clearly identified forest affected by hydrocarbons.

Not all indices sensitive to photosynthetic pigments were useful – MCARI index showed insensitive to chlorophyll content across multiple species. REP indices did not show a strong significant difference in polluted and non-polluted sites which contradicts the findings presented in other studies (Noomen & Skidmore 2009, Yang 1999, Smith;Steven & Colls 2004, Smith;Steven & Colls 2004, Yang et al. 2000). Vegetation indices using the blue range (EVI, ARVI, mSR_{705}, $mNDVI_{705}$) were not able to discriminate vegetation stress in the study sites due to the fact the low reflectance signal of the Hyperion images in this range of the spectrum. Vegetation indices related to other plant pigments consistently show lower values for pristine forest but they were not differentiating between polluted and non-polluted secondary forest. Three water content indices (NDWI, MSI and NDII) were able to detect higher levels of foliar water content in the site affected by hydrocarbons (Figure 9) as field data suggested.

The three indices of most use for mapping (explaining 83% of separability between the three sites), were the SG, NDVI and NDVI705, and are a mixture of both multispectral and hyperspectral vegetation indices. This particular selection of indices seems to be based on their ability to highlight lower levels of photosynthetic pigments, in particular chlorophyll (SG index) and dense vegetation with the high LAI (NDVI) characteristic of tropical forest environments. To employ these indices within a

monitoring system to detect petroleum contamination is attractive, particularly given the imminent improvements in sensor technology (e.g., launch of Sentinels) and capability and the simplicity of using the spectra measured by these sensors. Although subsequent studies are required to attain a greater insight into determining the relationship between the key foliar biochemicals, spectral response and levels of pollutant that can be detected, this is the first study to show that such a link holds promise and has been enabled by the intensive fieldwork undertaken.

5. Conclusions

This paper provides evidence of leaf biochemical alterations in the rainforest caused by petroleum pollution and demonstrates that these can be detected by spaceborne satellite remote sensing. The results indicate that tropical forests exposed to petroleum pollution show principally reduced levels of chlorophyll content, accompanied by higher levels of foliar water content. These alterations were detectable from space using the EO-1 Hyperion sensor by way of vegetation indices that are sensitive to detection changes of photosynthetic activity of the forest based on chlorophyll content and indices related to canopy density and vegetation vigour. This investigation has shown a potential for the use of imaging spectrometers for the identification and characterisation of hydrocarbon pollution or seep in dense tropical forests.

Acknowledgements

This research has been self-funded by the corresponding author and has the support of the Secretariat for Science and Technology of Ecuador (SENESCYT). We thank the Environmental Ministry of Ecuador for providing environmental studies and the Environmental Program for Pollution Remediation-PRAS for providing digital maps

and RAPID EYE satellite images of the study area. H. Balzter was supported by the Royal Society Wolfson Research Merit Award, 2011/R3 and the NERC National Centre for Earth Observation.

REFERENCES

Apan, A., Held, A., Phinn, S. & Markley, J. 2004, "Detecting sugarcane 'orange rust' disease using EO-1 Hyperion hyperspectral imagery", *International Journal of Remote Sensing,* vol. 25, no. 2, pp. 489-498.

Asner, G.P., Nepstad, D., Cardinot, G. & Ray, D. 2004, "Drought stress and carbon uptake in an Amazon forest measured with spaceborne imaging spectroscopy", *Proceedings of the National Academy of Sciences of the United States of America,* vol. 101, no. 16, pp. 6039-6044.

Baker, J.M. 1970, "The effects of oil on plants", *Environmental Pollution,* vol. 1, pp. 27-44.

Bernal, A.M. 2011, "Power, powerlessness and petroleum: Indigenous environmental claims and the limits of transnational law", *New Political Science,* vol. 33, no. 2, pp. 143-167.

Blackburn, G.A. 2007, "Hyperspectral remote sensing of plant pigments", *Journal of Experimental Botany,* vol. 58, no. 4, pp. 855-867.

Blackburn, G.A. 1998, "Spectral indices for estimating photosynthetic pigment concentrations: A test using senescent tree leaves", *International Journal of Remote Sensing,* vol. 19, no. 4, pp. 657-675.

Boyd, D.S., Entwistle, J.A., Flowers, A.G., Armitage, R.P. & Goldsmith, P.C. 2006, "Remote sensing the radionuclide contaminated Belarusian landscape: A potential for imaging spectrometry?", *International Journal of Remote Sensing,* vol. 27, no. 10, pp. 1865-1874.

Carter, G.A. 1994, "Ratios of leaf reflectances in narrow wavebands as indicators of plant stress", *International Journal of Remote Sensing,* vol. 15, no. 3, pp. 697-703.

Carter, G.A., Cibula, W.G. & Miller, R.L. 1996, "Narrow-band Reflectance Imagery Compared with ThermalImagery for Early Detection of Plant Stress", *Journal of Plant Physiology,* vol. 148, no. 5, pp. 515-522.

Curran, P.J. & Dash, J. 2005, *Algorithm theoretical basis document ATBD 2.2: chlorophyll index,* University of Southampton, Southampton-UK.

Dadon, A., Ben-Dor, E. & Karnieli, A. 2010, "Use of Derivative Calculations and Minimum Noise Fraction Transform for Detecting and Correcting the Spectral Curvature Effect (Smile) in Hyperion Images", *Geoscience and Remote Sensing, IEEE Transactions on*, vol. 48, no. 6, pp. 2603-2612.

Dash, J. & Curran, P.J. 2006, "Relationship between herbicide concentration during the 1960s and 1970s and the contemporary MERIS Terrestrial Chlorophyll Index (MTCI) for southern Vietnam", *International Journal of Geographical Information Science*, vol. 20, no. 8, pp. 929-939.

Datt, B. 1999, "Remote sensing of water content in Eucalyptus leaves", *Australian Journal of Botany*, vol. 47, no. 6, pp. 909-923.

Datt, B., McVicar, T.R., Van Niel, T.G., Jupp, D.L.B. & Pearlman, J.S. 2003, "Preprocessing EO-1 Hyperion hyperspectral data to support the application of agricultural indexes", *IEEE Transactions on Geoscience and Remote Sensing*, vol. 41, no. 6 PART I, pp. 1246-1259.

Daughtry, C.S.T., Walthall, C.L., Kim, M.S., de Colstoun, E.B. & McMurtrey III, J.E. 2000, "Estimating Corn Leaf Chlorophyll Concentration from Leaf and Canopy Reflectance", *Remote Sensing of Environment*, vol. 74, no. 2, pp. 229-239.

Davids, C. & Tyler, A.N. 2003, "Detecting contamination-induced tree stress within the Chernobyl exclusion zone", *Remote Sensing of Environment*, vol. 85, no. 1, pp. 30-38.

Davidson, E.A., De Araüjo, A.C., Artaxo, P., Balch, J.K., Brown, I.F., C. Bustamante, M.M., Coe, M.T., Defries, R.S., Keller, M., Longo, M., Munger, J.W., Schroeder, W., Soares-Filho, B.S., Souza Jr., C.M. & Wofsy, S.C. 2012, "The Amazon basin in transition", *Nature*, vol. 481, no. 7381, pp. 321-328.

Dawson, T.P. & Curran, P.J. 1998, "A new technique for interpolating the reflectance red edge position", *International Journal of Remote Sensing*, vol. 19, no. 11, pp. 2133-2139.

Environmental Ministry of Ecuador 2014, *Geoinformation survey for petroleum pollution sources*, Social and Environmental Program for Petroleum Pollution Remediation-PRAS, Quito-Ecuador.

Environmental Ministry of Ecuador 2009, *Auditoria ambiental bianual de las actividades hydrocarburiferas en el Bloque Tarapoa, campos compartidos Fanny 18B y Mariann 4A, las facilidades LTF en Lago Agrio y de cambio de operador de ARC Ecuador Ltd., a Andes Petroleum Ecuador Ltd.*, ENTRIX, Quito-Ecuador.

Environmental Ministry of Ecuador 2005, *Auditoria ambiental externa de las actividades hidrocarburiferas en el Bloque Tarapoa y el campo compartido Fanny 18B*, Walsh Environment Scientists and Engineers, Quito-Ecuador.

Féret, J., François, C., Gitelson, A., Asner, G.P., Barry, K.M., Panigada, C., Richardson, A.D. & Jacquemoud, S. 2011, "Optimizing spectral indices and chemometric

analysis of leaf chemical properties using radiative transfer modeling", *Remote Sensing of Environment,* vol. 115, no. 10, pp. 2742-2750.

Finer, M., Jenkins, C.N., Pimm, S.L., Keane, B. & Ross, C. 2008, "Oil and gas projects in the Western Amazon: Threats to wilderness, biodiversity, and indigenous peoples", *PLoS ONE,* vol. 3, no. 8.

Gamon, J.A., Peñuelas, J. & Field, C.B. 1992, "A narrow-waveband spectral index that tracks diurnal changes in photosynthetic efficiency", *Remote Sensing of Environment,* vol. 41, no. 1, pp. 35-44.

Gamon, J.A. & Surfus, J.S. 1999, "Assessing leaf pigment content and activity with a reflectometer", *New Phytologist,* vol. 143, no. 1, pp. 105-117.

Gao, B.-. 1996, "NDWI - A normalized difference water index for remote sensing of vegetation liquid water from space", *Remote Sensing of Environment,* vol. 58, no. 3, pp. 257-266.

Gerber, F., Marion, R., Olioso, A., Jacquemoud, S., Ribeiro da Luz, B. & Fabre, S. 2011, "Modeling directional–hemispherical reflectance and transmittance of fresh and dry leaves from 0.4 μm to 5.7 μm with the PROSPECT-VISIR model", *Remote Sensing of Environment,* vol. 115, no. 2, pp. 404-414.

Gitelson, A.A., Kaufman, Y.J. & Merzlyak, M.N. 1996, "Use of a green channel in remote sensing of global vegetation from EOS- MODIS", *Remote Sensing of Environment,* vol. 58, no. 3, pp. 289-298.

Gitelson, A.A. & Merzlyak, M.N. 1997, "Remote estimation of chlorophyll content in higher plant leaves", *International Journal of Remote Sensing,* vol. 18, no. 12, pp. 2691-2697.

Gitelson, A.A., Merzlyak, M.N. & Chivkunova, O.B. 2001, "Optical properties and nondestructive estimation of anthocyanin content in plant leaves", *Photochemistry and photobiology,* vol. 74, no. 1, pp. 38-45.

Goodenough, D.G., Dyk, A., Niemann, K.O., Pearlman, J.S., Chen, H., Han, T., Murdoch, M. & West, C. 2003, "Processing Hyperion and ALI for forest classification", *IEEE Transactions on Geoscience and Remote Sensing,* vol. 41, no. 6 PART I, pp. 1321-1331.

Goodenough, D.G., Quinn, G.S., Gordon, P.L., Niemann, K.O. & Chen, H. 2011, "Linear and nonlinear imaging spectrometer denoising algorithms assessed through chemistry estimation", , pp. 4320.

Guyot, G., Baret, F. & Major, D.J. 1988, "High spectral resolution: Determination of spectral shifts between the red and the near infrared", *International Archives of Photogrammetry and Remote Sensing,* vol. 11, pp. 740-760.

Hardisky, M.A., Klemas, V. & Smart, R.M. 1983, "The influence of soil salinity, growth form, and leaf moisture on the spectral radiance of *Spartina alterniflora*

canopies.", *Photogrammetric Engineering & Remote Sensing,* vol. 49, no. 1, pp. 77-83.

Hoel, B.O. 1998, "Use of a hand-held chlorophyll meter in winter wheat: Evaluation of different measuring positions on the leaves", *Acta Agriculturae Scandinavica - Section B Soil and Plant Science,* vol. 48, no. 4, pp. 222-228.

Horvitz, L. 1982, "Near-surface evidence of hydrocarbon movement from depth" in *Problems of petroleum migration,* eds. W.H. Roberts & R.J. Cordell, AAPG Studies in Geology 10 edn, American Association of Petroluem Geologists, Tulsa, Oklahoma, USA, pp. 241-263.

Horvitz, L. 1985, "Geochemical exploration for petroleum", *Science,* vol. 229, no. 4716, pp. 821-827.

Huete, A.R., Liu, H.Q., Batchily, K. & Van Leeuwen, W. 1997, "A comparison of vegetation indices over a global set of TM images for EOS-MODIS", *Remote Sensing of Environment,* vol. 59, no. 3, pp. 440-451.

Hunt Jr, E.R. & Rock, B.N. 1989, "Detection of changes in leaf water content using Near- and Middle-Infrared reflectances", *Remote Sensing of Environment,* vol. 30, no. 1, pp. 43-54.

Hurtig, A.K. & San-Sebastián, M. 2005, "Epidemiology vs epidemiology: The case of oil exploitation in the Amazon basin of Ecuador [5]", *International journal of epidemiology,* vol. 34, no. 5, pp. 1170-1172.

Jago, R.A., Cutler, M.E.J. & Curran, P.J. 1999, "Estimating canopy chlorophyll concentration from field and airborne spectra", *Remote Sensing of Environment,* vol. 68, no. 3, pp. 217-224.

Kaufman, Y.J. & Tanre, D. 1992, "Atmospherically resistant vegetation index (ARVI) for EOS-MODIS", *IEEE Transactions on Geoscience and Remote Sensing,* vol. 30, no. 2, pp. 261-270.

Kooistra, L., Leuven, R.S.E.W., Wehrens, R., Nienhuis, P.H. & Buydens, L.M.C. 2003, "A comparison of methods to relate grass reflectance to soil metal contamination", *International Journal of Remote Sensing,* vol. 24, no. 24, pp. 4995-5010.

Larcher, W. 2003, *Physiological Plant Ecology,* Fourth edn, Spinger, Germany.

Lichtenthaler, H.K., Lang, M., Sowinska, M., Heisel, F. & Miehé, J.A. 1996, "Detection of vegetation stress via a new high resolution fluorescence imaging system", *Journal of Plant Physiology,* vol. 148, no. 5, pp. 599-612.

Malhi, Y., Roberts, J.T., Betts, R.A., Killeen, T.J., Li, W. & Nobre, C.A. 2008, "Climate change, deforestation, and the fate of the Amazon", *Science,* vol. 319, no. 5860, pp. 169-172.

641 Marenco, R.A., Antezana-Vera, S.A. & Nascimento, H.C.S. 2009, "Relationship
642 between specific leaf area, leaf thickness, leaf water content and SPAD-502
643 readings in six Amazonian tree species", *Photosynthetica*, vol. 47, no. 2, pp. 184-
644 190.

645 Martin, P.L. 2011, "Global governance from the amazon: Leaving oil underground in
646 Yasuní National park, Ecuador", *Global Environmental Politics*, vol. 11, no. 4, pp.
647 22-42.

648 Marx, E. 2010, "The fight for Yasuni", *Science*, vol. 330, no. 6008, pp. 1170-1171.

649 Ministerio de Energia y Minas 2001, *Reglamento Ambiental para Operaciones*
650 *Hidrocarburiferas en el Ecuador*, Decreto Ejecutivo 1215 edn, Registro oficial
651 265, Ecuador.

652 Mutanga, O., Skidmore, A.K. & Prins, H.H.T. 2004, "Predicting in situ pasture quality
653 in the Kruger National Park, South Africa, using continuum-removed absorption
654 features", *Remote Sensing of Environment*, vol. 89, no. 3, pp. 393-408.

655 Noomen, M.F. 2007, *Hyperspectral Reflectance of vegetation affected by underground*
656 *hydrocarbon gas seepage*, PhD edn, International Institute for Geo-Information
657 Science & Earth Observation-ITC, Enschede-The Netherlands.

658 Noomen, M.F. & Skidmore, A.K. 2009, "The effects of high soil CO2 concentrations on
659 leaf reflectance of maize plants", *International Journal of Remote Sensing*, vol. 30,
660 no. 2, pp. 481-497.

661 Noomen, M.F., Skidmore, A.K., van der Meer, F.D. & Prins, H.H.T. 2006, "Continuum
662 removed band depth analysis for detecting the effects of natural gas, methane and
663 ethane on maize reflectance", *Remote Sensing of Environment*, vol. 105, no. 3, pp.
664 262-270.

665 Noomen, M.F., Smith, K.L., Colls, J.J., Steven, M.D., Skidmore, A.K. & Van Der
666 Meer, F.D. 2008, "Hyperspectral indices for detecting changes in canopy
667 reflectance as a result of underground natural gas leakage", *International Journal*
668 *of Remote Sensing*, vol. 29, no. 20, pp. 5987-6008.

669 Noomen, M.F., van der Werff, H.M.A. & van der Meer, F.D. 2012, "Spectral and
670 spatial indicators of botanical changes caused by long-term hydrocarbon seepage",
671 *Ecological Informatics*, vol. 8, pp. 55-64.

672 Penuelas, J., Filella, I., Lloret, P., Munoz, F. & Vilajeliu, M. 1995, "Reflectance
673 assessment of mite effects on apple trees", *International Journal of Remote*
674 *Sensing*, vol. 16, no. 14, pp. 2727-2733.

675 Peñuelas, J., Piñol, J., Ogaya, R. & Filella, I. 1997, "Estimation of plant water
676 concentration by the reflectance Water Index WI (R900/R970)", *International*
677 *Journal of Remote Sensing*, vol. 18, no. 13, pp. 2869-2875.

678 Pimstein, A., Eitel, J.U.H., Long, D.S., Mufradi, I., Karnieli, A. & Bonfil, D.J. 2009, "A
679 spectral index to monitor the head-emergence of wheat in semi-arid conditions",
680 *Field Crops Research*, vol. 111, no. 3, pp. 218-225.

681 Rochlin, J. 2011, "Development, the environment and ecuador's oil patch: The context
682 and nuances of the case against Texaco", *Journal of Third World Studies*, vol. 28,
683 no. 2, pp. 11-39.

684 Rondeaux, G., Steven, M. & Baret, F. 1996, "Optimization of soil-adjusted vegetation
685 indices", *Remote Sensing of Environment*, vol. 55, no. 2, pp. 95-107.

686 Rosso, P.H., Pushnik, J.C., Lay, M. & Ustin, S.L. 2005, "Reflectance properties and
687 physiological responses of Salicornia virginica to heavy metal and petroleum
688 contamination", *Environmental Pollution*, vol. 137, no. 2, pp. 241-252.

689 Rouse, J.W., Haas, R.H. & Schell, J.A. 1974, "Monitoring the Vernal Advancement of
690 Retrogradiation of Natural Vegetation", .

691 Sánchez-Azofeifa, G.A., Castro, K., Wright, S.J., Gamon, J., Kalacska, M., Rivard, B.,
692 Schnitzer, S.A. & Feng, J.L. 2009, "Differences in leaf traits, leaf internal structure,
693 and spectral reflectance between two communities of lianas and trees: Implications
694 for remote sensing in tropical environments", *Remote Sensing of Environment*, vol.
695 113, no. 10, pp. 2076-2088.

696 Shumacher, D. 1996, "*Hydrocarbon-induced alteration of soils and sediments*" in
697 *Hydrocarbon migration and its near-surface expression: APPG Memoir 66*, eds. D.
698 Shumacher & M.A. Abrams, pp. 71-89.

699 Sims, D.A. & Gamon, J.A. 2002, *Relationships between leaf pigment content and*
700 *spectral reflectance across a wide range of species, leaf structures and*
701 *developmental stages*.

702 Smith, K.L., Steven, M.D. & Colls, J.J. 2004, "Remote sensing techniques for
703 monitoring plant stress responses to gas leaks", *International Gas Research*
704 *Conference Proceedings*, .

705 Smith, K.L., Colls, J.J. & Steven, M.D. 2005, *A Facility to Investigate Effects of*
706 *Elevated Soil Gas Concentration on Vegetation*, Springer Netherlands.

707 Smith, K.L., Steven, M.D. & Colls, J.J. 2005, "Plant spectral responses to gas leaks and
708 other stresses", *International Journal of Remote Sensing*, vol. 26, no. 18, pp. 4067.

709 Smith, K.L., Steven, M.D. & Colls, J.J. 2004, "Use of hyperspectral derivative ratios in
710 the red-edge region to identify plant stress responses to gas leaks", *Remote Sensing*
711 *of Environment*, vol. 92, no. 2, pp. 207-217.

712 Steven, M.D., Malthus, T.J., Demetriades-Shah, T.H., Danson, F.M. & Clark, J.A.
713 1990, "High-spectral resolution indices for crop stress", *Applications of remote*
714 *sensing in agriculture*, , pp. 209-227.

715 Tedersoo, L., Sadam, A., Zambrano, M., Valencia, R. & Bahram, M. 2010, "Low
716 diversity and high host preference of ectomycorrhizal fungi in Western Amazonia,
717 a neotropical biodiversity hotspot", *ISME Journal*, vol. 4, no. 4, pp. 465-471.

718 Vallejo, M.C., Burbano, R., Falconí, F. & Larrea, C. 2015, "Leaving oil underground in
719 Ecuador: The Yasuní-ITT initiative from a multi-criteria perspective", *Ecological*
720 *Economics*, vol. 109, no. 0, pp. 175-185.

721 van der Meer, F., Yang, H. & Kroonenberg, S. 2006, "Imaging spectrometry and
722 petroleum geology" in *Imaging Spectrometry*, eds. F. van der Meer & S.M. de
723 Jong, Springer, Dordrecht, The Netherlands, pp. 219-241.

724 Vile, D., Garnier, É., Shipley, B., Laurent, G., Navas, M.-., Roumet, C., Lavorel, S.,
725 Díaz, S., Hodgson, J.G., Lloret, F., Midgley, G.F., Poorter, H., Rutherford, M.C.,
726 Wilson, P.J. & Wright, I.J. 2005, "Specific leaf area and dry matter content
727 estimate thickness in laminar leaves", *Annals of Botany*, vol. 96, no. 6, pp. 1129-
728 1136.

729 Vogelmann, J.E., Rock, B.N. & Moss, D.M. 1993, "Red edge spectral measurements
730 from sugar maple leaves", *International Journal of Remote Sensing*, vol. 14, no. 8,
731 pp. 1563-1575.

732 White, J.W. & Montes-R, C. 2005, "Variation in parameters related to leaf thickness in
733 common bean (Phaseolus vulgaris L.)", *Field Crops Research*, vol. 91, no. 1, pp. 7-
734 21.

735 Yang, H. 1999, *Imagining Spectrometry for Hydrocarbon Microseepage*, Delf
736 University of Technology.

737 Yang, H., Zhang, J., Van Der Meer, F. & Kroonenberg, S.B. 2000, "Imaging
738 spectrometry data correlated to hydrocarbon microseepage", *International Journal*
739 *of Remote Sensing*, vol. 21, no. 1, pp. 197-202.

740 Zarco-Tejada, P.J., Miller, J.R., Mohammed, G.H. & Noland, T.L. 2000, "Chlorophyll
741 fluorescence effects on vegetation apparent reflectance: I. Leaf-level measurements
742 and model simulation", *Remote Sensing of Environment*, vol. 74, no. 3, pp. 582-
743 595.

744 Zhu, L., Zhao, X., Lai, L., Wang, J., Jiang, L., Ding, J., Liu, N., Yu, Y., Li, J., Xiao, N.,
745 Zheng, Y. & Rimmington, G.M. 2013, "Soil TPH Concentration Estimation Using
746 Vegetation Indices in an Oil Polluted Area of Eastern China", *PLoS ONE*, vol. 8,
747 no. 1.

748 Zweifel, R., Rigling, A. & Dobbertin, M. 2009, *Species-specific stomatal response of*
749 *trees to drought - A link to vegetation dynamics?*.

750